Original Research

Quantitative Myocardial Infarction on Delayed Enhancement MRI. Part I: Animal Validation of an Automated Feature Analysis and Combined Thresholding Infarct Sizing Algorithm

Li-Yueh Hsu, DSc, Alex Natanzon, MD, Peter Kellman, PhD, Glenn A. Hirsch, MD, Anthony H. Aletras, PhD, and Andrew E. Arai, MD*

Purpose: To develop a computer algorithm to measure myocardial infarct size in gadolinium-enhanced magnetic resonance (MR) imaging and to validate this method using a canine histopathological reference.

Materials and Methods: Delayed enhancement MR was performed in 11 dogs with myocardial infarction (MI) determined by triphenyltetrazolium chloride (TTC). Infarct size on in vivo and ex vivo images was measured by a computer algorithm based on automated feature analysis and combined thresholding (FACT). For comparison, infarct size by human manual contouring and simple intensity thresholding (based on two standard deviation [2SD] and full width at half maximum [FWHM]) were studied.

Results: Both in vivo and ex vivo MR infarct size measured by the FACT algorithm correlated well with TTC (R = 0.95–0.97) and showed no significant bias on Bland Altman analysis (P = not significant). Despite similar correlations (R = 0.91–0.97), human manual contouring overestimated in vivo MR infarct size by 5.4% of the left ventricular (LV) area (equivalent to 55.1% of the MI area) vs. TTC ($P < 0.001$). Infarct size measured by simple intensity thresholdings was less accurate than the proposed algorithm ($P < 0.001$ and $P = 0.007$).

Conclusion: The FACT algorithm accurately measured MI size on delayed enhancement MR imaging in vivo and ex vivo. The FACT algorithm was also more accurate than human manual contouring and simple intensity thresholding approaches.

Key Words: myocardial infarction; magnetic resonance imaging; computer algorithm; image processing; expert system; contrast agent; gadolinium
J. Magn. Reson. Imaging 2006;23:298–308.
Published 2006 Wiley-Liss, Inc.†

THERE IS A NEED to develop objective image analysis methods that can accurately quantify the size of myocardial infarction (MI) on delayed enhancement magnetic resonance (MR) images. Landmark studies of Kim et al (1) and Fieno et al (2) validated that gadolinium delayed contrast-enhancement closely tracks the area of irreversible myocardial injury due to acute or chronic infarction. However, these studies did not evaluate the accuracy of in vivo images, did not use the inversion recovery techniques (3) popular for clinical exams, and only validated ex vivo images obtained at resolutions that are currently impractical in patients ($0.5 \times 0.5 \times 0.5$ mm). Furthermore, quantification of MI in these studies were based on an empirical simple intensity thresholding of more than two SD (2SD) (1) or more than three SD (3SD) (2) above the mean of the normal myocardial intensity for infarct size measurements.

Prior studies suggested errors in estimating infarct size may be partially explained by slice thickness and partial volume effects (1,4–6). Quantification of MI size has been performed using human manual contouring and by computerized simple intensity thresholding based on the SD of normal myocardial signal intensities (1,2,7–12). Considering partial volume effects, an alternative threshold value at 50% of the maximum intensity, sometimes referred as full width at half maximum (FWHM) (13), theoretically should be more accurate to dichotomize normal and infarcted myocardial pixels. Although simple intensity thresholding techniques reduce intraobserver or interobserver variability compared to human manual contouring, they lack robustness due to the use of empirical thresholds, varied bight pixel intensity across different myocardial regions, and surface coil intensity variation.

Laboratory of Cardiac Energetics, National Heart Lung and Blood Institute, National Institutes of Health, Department of Health and Human Services, Bethesda, Maryland, USA.

Contract grant sponsor: National Heart, Lung, and Blood Institute, National Institutes of Health.

*Address reprint requests to: A.E.A., Laboratory of Cardiac Energetics, National Heart, Lung, and Blood Institute, National Institutes of Health, 10 Center Dr., MSC 1061, Building 10, Room B1D-416, Bethesda, MD 20892-1061. E-mail: araia@nih.gov

Received February 19, 2005; Accepted October 28, 2005.
DOI 10.1002/jmri.20496
Published online 31 January 2006 in Wiley InterScience (www.interscience.wiley.com).

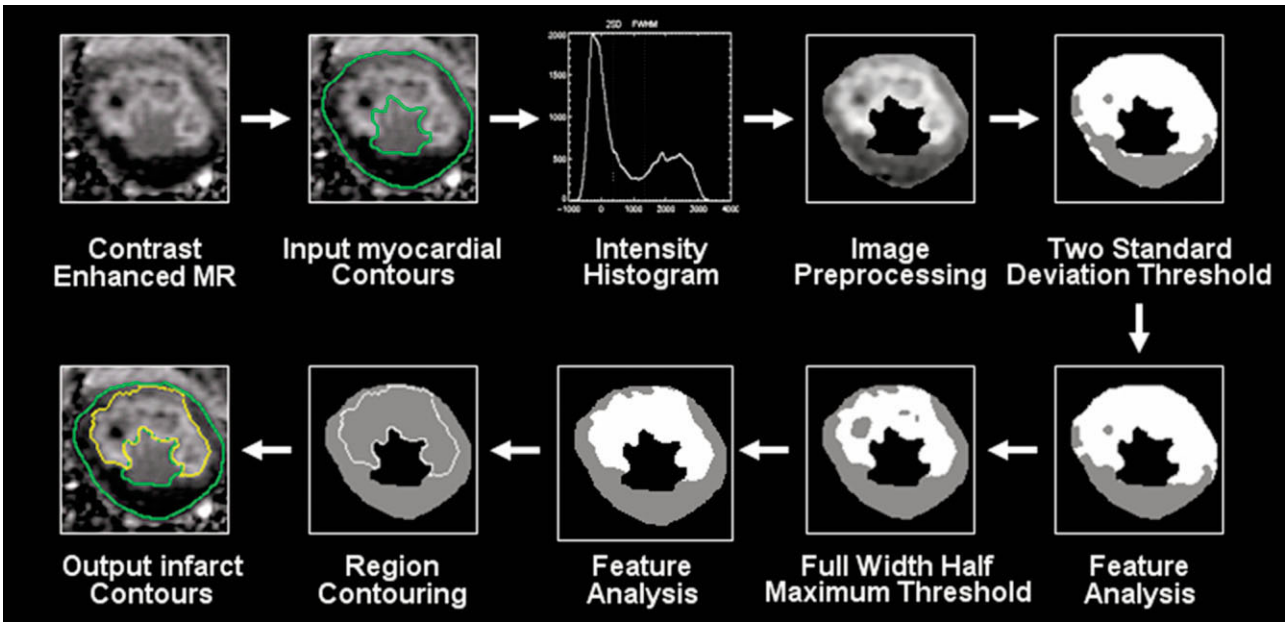

Figure 1. Data flow of the FACT infarct sizing algorithm. After manual segmentation of epicardial and endocardial borders, the algorithm automatically selects optimal intensity thresholds, performs region-based feature analysis, compensates microvascular obstruction areas, and finally contours the contrast-enhanced regions of interest.

Thus, the purpose of this study was to develop a computer algorithm to improve MI size measurement in gadolinium-enhanced MR imaging and to validate this method using a canine histopathological reference. We hypothesized that computer algorithms that incorporate expert knowledge (expert system) could objectively analyze infarct regions with user independent thresholds, and advanced image processing techniques that use feature analysis to eliminate false positive bright regions and to compensate dark areas of microvascular obstruction. Such a system should be more accurate than human manual contouring or simple intensity thresholding. It is particularly beneficial if these methods were validated on images acquired with practical in vivo resolution.

MATERIALS AND METHODS

Study Design

After developing the feature analysis and combined thresholding (FACT) computer expert system for measuring infarct size on delayed enhancement images, an animal model with triphenyltetrazolium chloride (TTC) histopathology was used to validate MR infarct size measured by the FACT algorithm and human manual contouring on both in vivo and ex vivo images. Intraobserver and interobserver agreements of the FACT algorithm and human manual contouring were assessed. Finally, the FACT algorithm and simple intensity thresholding methods (based on 2SD and FWHM) were compared against the TTC reference standard.

FACT Algorithm

Figure 1 illustrates graphically how the FACT infarct sizing algorithm applied a series of pre-determined steps to automatically calculate intensity thresholds, perform feature analysis, and classify infarcted and normal pixels. The algorithm analyzed image features derived from expert knowledge to exclude false positive areas such as discrete bright patches that were not contiguous with other bright regions. Additional post-processing procedures were applied to include areas of microvascular obstruction. For all images, the epicardial and endocardial borders were manually contoured using custom image display and analysis software written in Interactive Display Language (Research Systems Inc., Boulder, CO, USA) before applying the FACT algorithm, which was implemented in Microsoft Visual C++ Language (Microsoft Corporation, Redmond, WA, USA).

Figure 2 shows the flow diagram of the FACT algorithm for myocardial infarct sizing. From the analysis of the pixel intensity histogram (Fig. 1), a bi-modal distribution is observed from the myocardial regions of interest. In contrast-enhanced infarct imaging with phase sensitive inversion recovery (PSIR) reconstruction (14) and surface coil intensity correction, normal myocardial pixel values appear in the low intensity portion of the histogram and follow a Gaussian distribution. Due to the T1 weighting of contrast enhancement, the infarct tissue values are at the higher intensity portion of the histogram.

The algorithm automatically estimated an initial threshold to separate the infarction from the normal myocardium. Both median filtering and histogram clustering (15) were used to smooth the random noise on the spatial and the histogram spaces before the threshold estimation.

2SD Thresholding

The mean and SD of the normal tissue intensities were first estimated by the maximum value of the lower part

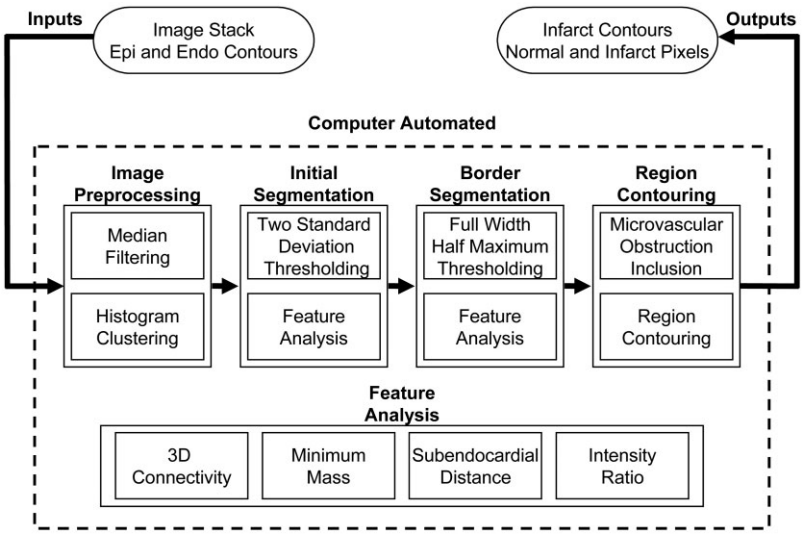

Figure 2. Flow diagram of the FACT infarct sizing algorithm. There are a series of image processing steps to classify the myocardial regions of interest into normal and infarct pixels.

of the intensity histogram. The threshold value was then calculated as 2 SD above the mean. Pixels darker than this threshold value were excluded from further analysis. This, however, left aggregates of bright pixels that included infarct, imperfectly excluded pixels of epicardial fat or right ventricular blood, randomly bright pixels, and potential artifacts. An initial threshold set at 2 SD above the mean may seem relatively low since it only covers 95% of a normal distribution. However, it is desirable to maintain a lower threshold to increase the probability of detecting more bright infarcts and then discounting false positive infarct pixels during follow up processing.

Region-Based Feature Analysis

To remove false positive pixels, the following image features were computed and classified on each aggregated potential infarct region in three-dimensional space: volume mass, subendocardial distance, and mean intensity. Before the feature analysis, all slices were registered to the center of the myocardial regions of interest. This ensures a proper three-dimensional propagation of myocardial regions through the entire image stack.

To calculate the infarct mass, all potential two-dimensional regions were first grouped to three-dimensional volumes using connected component analysis (15). This technique aggregates isolated two-dimensional regions into three-dimensional volumes based on the definition of neighbor connectivity. We implemented a 10-neighbor connectivity based on the large slice thickness of our dataset. After the process, each potential three-dimensional volume was then converted to units of mass based on the density of myocardium (1.05 g/mm^3). Any bright volume that had a mass smaller than a minimum setting (0.1 g) was considered as noise and removed.

To obtain the subendocardial distance, the shortest path of each potential three-dimensional infarcted volume to the endocardial boundary was computed amongst all border pixels. Any bright volume more than 2 mm away from the endocardial border was considered a potential artifact and removed. Additionally, the intensity value of each potential three-dimensional volume was examined for homogeneity. For each volume, the mean intensity value was computed as a ratio to the average intensity of all potential infarcted volumes. A minimum setting of 50% was used to remove volumes that have a darker average intensity.

FWHM Thresholding

While the above steps effectively remove disjointed false positive bright regions, overestimation of infarct size is still possible due to the tissue partial volume effect. The next step was to determine a final threshold to classify partial volume tissues. We defined a 50% of the maximum intensity threshold as the mid point between the average normal myocardial pixel intensity and the peak infarct pixel intensity. Any residual bright pixels less than this value were excluded from the infarct region of interest. After the thresholding, the region-based feature analysis was repeated to further reduce false positive infarct regions.

Inclusion of Microvascular Obstruction

Additional post-processing steps were applied to take account of dark pixel regions that may represent microvascular obstruction. An image morphology closing operation (15) with a crossbar shape kernel was used to connect small concave borders and fill small dark cavities surrounded by bright infarcted pixels. A small kernel (5 mm) of such process can also smooth the border of infarct regions without excessively altering the overall shape. Next, remaining regions of isolated dark pixels were further analyzed to identify possible areas of microvascular obstruction. Each dark region was reclassified as infarct if its border was completely encompassed by either endocardial or infarct pixels. These processes compensated for dark areas of microvascular obstruction that were too low in signal intensity to be classified as infarct by the thresholding steps. Finally, an edge-following step using an m-neighbor path (15) was applied to obtain the contour of infarcted regions for qualitative representation.

Animal Preparation

Eleven mongrel dogs (average weight 18 kg) underwent a 90-minute occlusion of the left anterior descending coronary artery in an open chest model followed by reperfusion. Five animals were imaged two days post-MI and six were studied two months post-MI. All procedures and imaging studies were approved by the Animal Care and Use Committee of the National Institutes of Health.

Image Acquisition

Infarct imaging was performed on a 1.5-T scanner (GE Medical Systems, Waukesha, WI, USA) approximately 20–30 minutes following gadolinium diethyltriaminepentaacetic acid (Gd-DTPA) administration using an inversion recovery fast gradient-echo sequence triggered every other heartbeat. Imaging used multiple two-dimensional acquisitions of the left ventricle (LV) in a short axis plane from base to apex. All images were corrected for surface coil intensity variation and used PSIR reconstruction (14). Typical imaging parameters of the study included TE 3.4 msec, TR 7.8 msec, approximately optimized inversion time (TI typically 300 msec), bandwidth ± 31.25 kHz, and acquisition time 125 msec per RR interval, which achieved a spatial resolution of $1.1 \times 1.8 \times 8.0$ mm in vivo and $0.6 \times 0.6 \times 4.0$ mm ex vivo.

Histopathology Preparation

MI was assessed on both in vivo and ex vivo MR images and compared with histopathology. Excised hearts were rinsed with normal saline and sliced into 4-mm sections using a commercial meat slicer (Globe Food Equipment, Dayton, OH, USA). Each slice was stained with TTC at 37°C for 5–10 minutes to demarcate the infarct territory. TTC stained slices were then submerged in 0.9% normal saline and photographed using a digital camera (Nikon D100, Melville, NY, USA) at a resolution about 0.065 mm per pixel. Epicardial, endocardial, and infarct borders were manually contoured by one observer. Both MR and TTC images were visually matched based on anatomic landmarks, which included LV shape, papillary muscle shape and location, and insertion point of the right ventricle. For each animal, five best-matched consecutive MR images with corresponding TTC slices were selected. Overall, 55 ex vivo MR-to-TTC and 55 in vivo MR-to-TTC image pairs were studied to validate and compare infarct size measurements by human manual contouring and various computerized methods.

Statistical Analysis

For comparison of infarct size measurements using the FACT algorithm, human manual contouring, and simple intensity thresholding methods, the same epicardial and endocardial contours of each slice were used to minimize bias. All the ex vivo and in vivo MR images were processed using the same computer parameter settings for the entire study.

Validations of the FACT algorithm and human manual contouring on both ex vivo and in vivo MR images against TTC were performed by two observers using linear correlation (16) and Bland Altman analysis (17). A paired t-test with Bonferroni correction for multiple comparisons was performed to determine if there was a significant difference ($P < 0.05$) between different methods. The result was reported as both percent of the LV area and percent of the MI area. The use of percent slice measurements was an important consideration in the intermodality comparison of MR-to-TTC to reduce registration error due to physiological distortions and during the histopathological preparation. TTC results were used as the independent variable for all analyses, and were taken as the reference standard for defining normal and infarcted myocardium.

Comparisons of intraobserver and interobserver variability were performed to test the reproducibility of the FACT algorithm and human manual contouring of infarct size on both ex vivo and in vivo MR images. The errors and differences in measuring infarct size were reported in both percent of LV area and percent of MI area using TTC as the reference standard. Intraobserver and interobserver agreements were also studied on a pixel-by-pixel comparison of infarcted and normal myocardium classifications using Cohen's kappa statistics (18).

Comparisons of the FACT algorithm vs. simple intensity thresholding techniques widely used by other studies (1,2,7–13) were performed to evaluate the efficacy of different computer based methods in infarct sizing. We compared 2SD intensity thresholding and FWHM intensity thresholding to the FACT algorithm, which combines both thresholdings and additional image feature analysis. The infarct size of ex vivo and in vivo MR images was studied using all these computerized methods and compared to the TTC reference standard.

RESULTS

Details at the edges of infarcts on TTC slices can appear blurred or disappear on MR due to the partial volume effect or motion, particularly on in vivo images (Fig. 3). Sample contours of a matched set of MR and TTC images show good agreement between the infarct region contoured by a human observer and the FACT algorithm (Fig. 4). Qualitatively, the shape and location of infarcted regions appear similar between human and computer contouring. The algorithm is also capable of following highly detailed infarct contours as shown on the example TTC image. However, the TTC reference standard used in MR validation was contoured by human planimetry.

Validations of the FACT Algorithm and Human Manual Contouring

Using the TTC measurements as the reference standard, the errors of either observer using the FACT algorithm and with manual planimetry to measure the MR infarct size were calculated in both percent of LV and percent of MI area. Since acute and chronic infarcts in our study exhibited similar correlation, slope, inter-

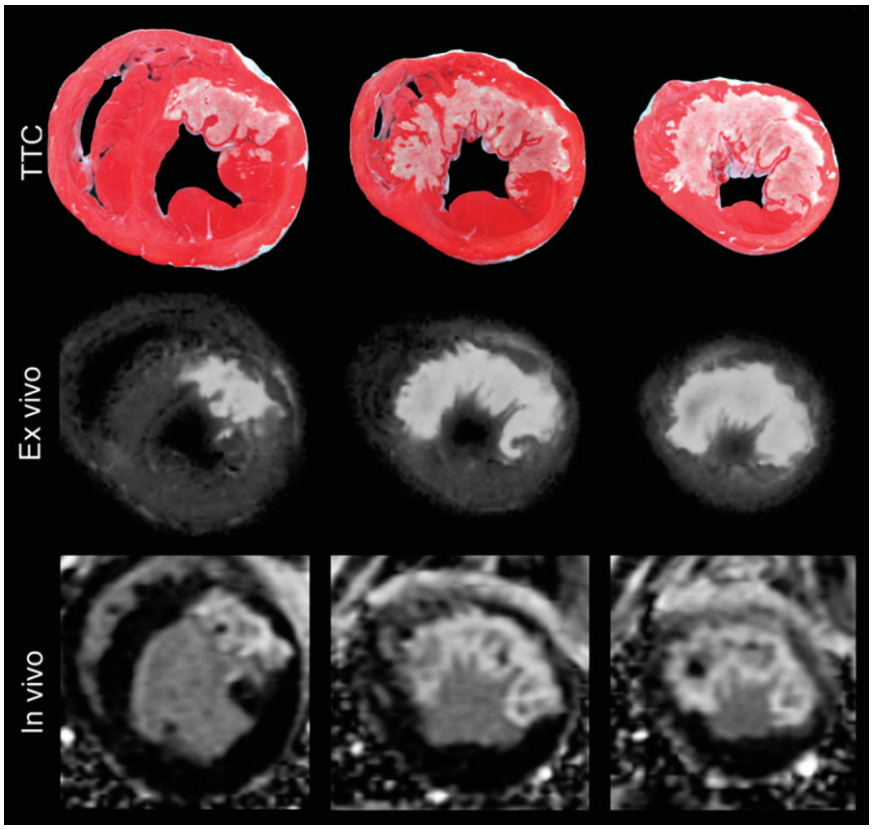

Figure 3. Despite good registration of MR with TTC, the lower spatial resolution of the in vivo image (in the middle) blurs details such as the hook shaped lateral edge of the infarct as evident on TTC and the ex vivo image (Dog 4).

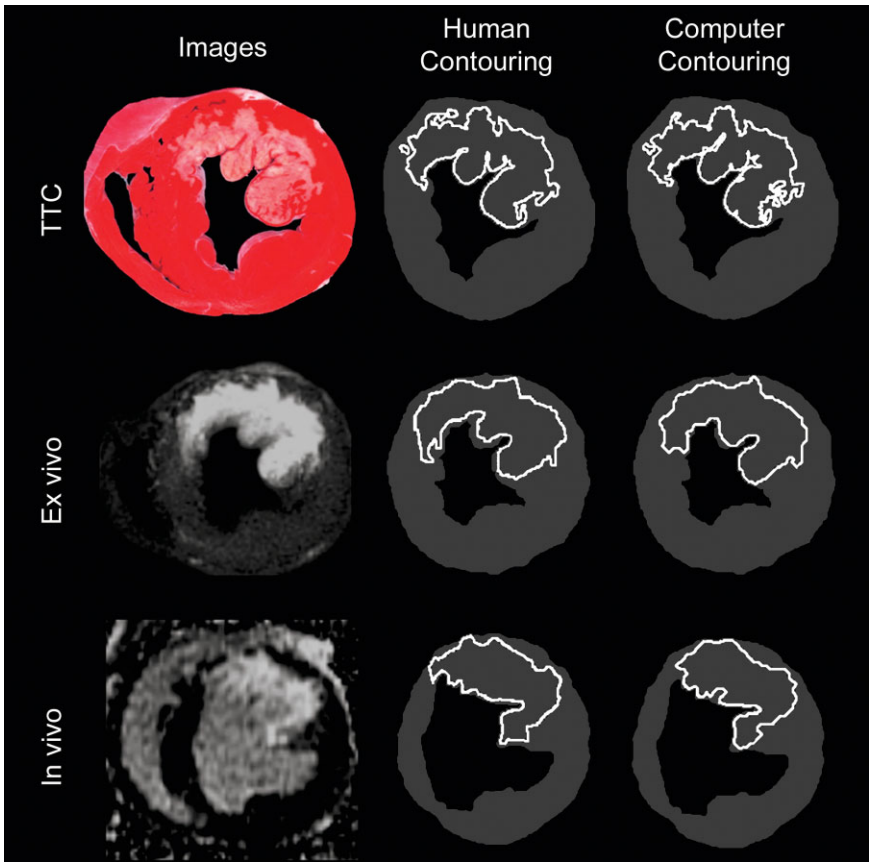

Figure 4. Examples of myocardial infarct borders contoured by human and computer (FACT) demonstrate that the algorithm is capable of highly detailed contours (Dog 6).

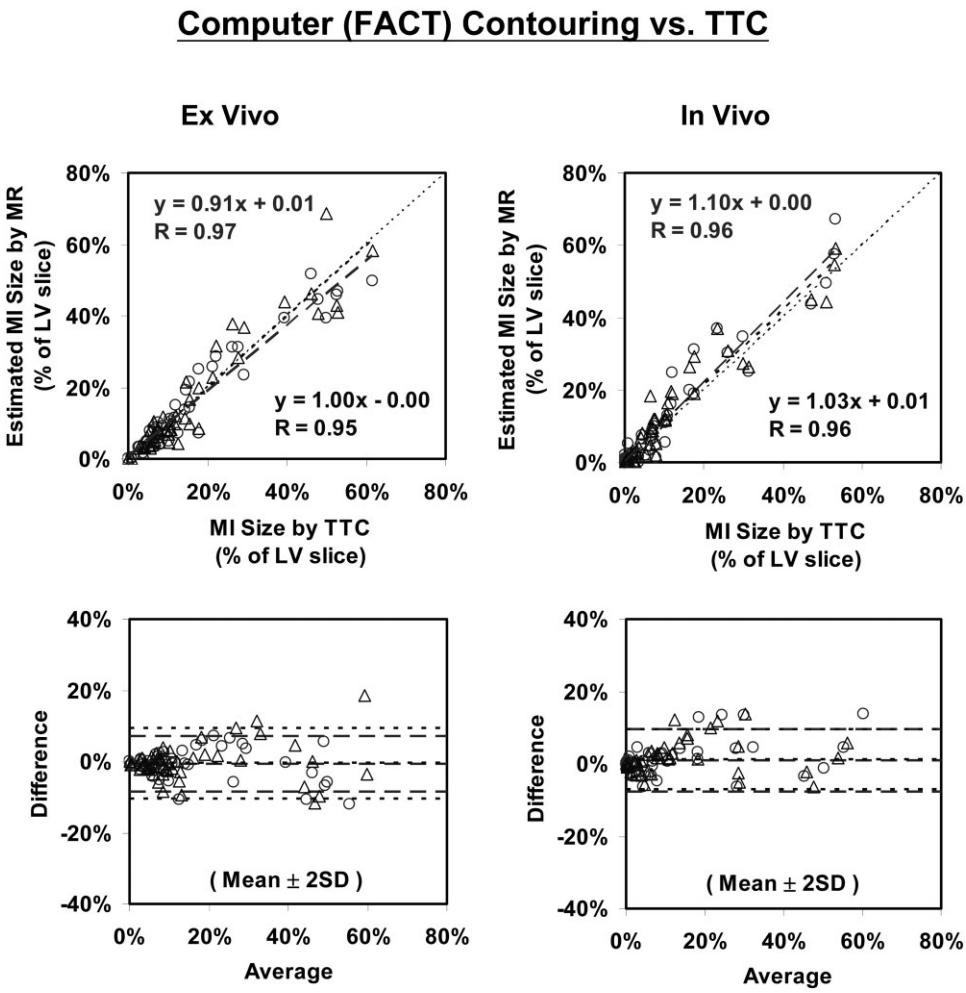

Figure 5. Ex vivo and in vivo MR infarct size measured by the computer (FACT) correlates well with TTC (intermodality comparison, MR vs. TTC). Bland Altman analysis shows no systematic bias. The first and second observers are indicated in open circles (dashed line) and triangles (dotted line), respectively.

cept, and scatter, all results were simplified by combining both data sets.

For the FACT algorithm, the correlations between overall infarct size on MR and the TTC reference standard were good for both in vivo and ex vivo images (Fig. 5, R = 0.95 to 0.97). Bland Altman analysis also showed no consistent bias as a function of infarct size. When results from a given animal were summarized into a single volumetric measurement, the correlations between FACT and TTC were even higher (ex vivo observer 1: y = 0.96x – 0.00, R = 0.99; ex vivo observer 2: y = 1.01x – 0.00, R = 0.98; in vivo observer 1: y = 1.05x + 0.01, R = 0.97; in vivo observer 2: y = 0.96x + 0.02, R = 0.98).

While good correlations (R = 0.91 to 0.97) between human manual contouring of infarct size on MR and TTC images were achieved (Fig. 6), human contouring overestimated infarct size on in vivo images. Bland Altman analysis also demonstrated relatively increased scatter from the human contouring. When results were summarized into global volumetric measurements, the correlations between human contouring and TTC were improved but still overestimated the infarct size (ex vivo observer 1: y = 0.99x + 0.03, R = 0.99; ex vivo observer 2: y = 1.03x + 0.03, R = 0.97; in vivo observer 1: y = 1.21x + 0.01, R = 0.97; in vivo observer 2: y = 1.07x + 0.05, R = 0.94).

There were even tighter correlations when comparing human measurements of infarct size with the FACT algorithm on the same MR images since there were no registration errors (Fig. 7). Although there was almost no difference between human and computer measurements of infarct size on ex vivo slices, human contouring of in vivo images overestimated infarct size when compared with the FACT algorithm.

While the error of human contouring using percent of the LV area as the measurement looks small relative to the entire ventricle, the error is considerably larger using the area of MI as the denominator. The human contouring of MR overestimated infarct size on ex vivo images by 3.2% of the LV (equivalent to 22.2% of the MI) area and to a greater degree on in vivo images by 5.4% of the LV (equivalent to 55.1% of the MI) area (all $P <$ 0.001 vs. TTC). Using the FACT algorithm, the average error was 0.5% of the LV (equivalent to 3.5% of the MI) area on ex vivo images, and 1.2% of the LV (equivalent to 11.9% of the MI) area on in vivo images (all P not significant vs. TTC).

Comparisons of Intraobserver and Interobserver Variability

Both observers had similar errors and moderate differences (1.2% of the LV, or 7.9% of the MI area, $P < 0.001$

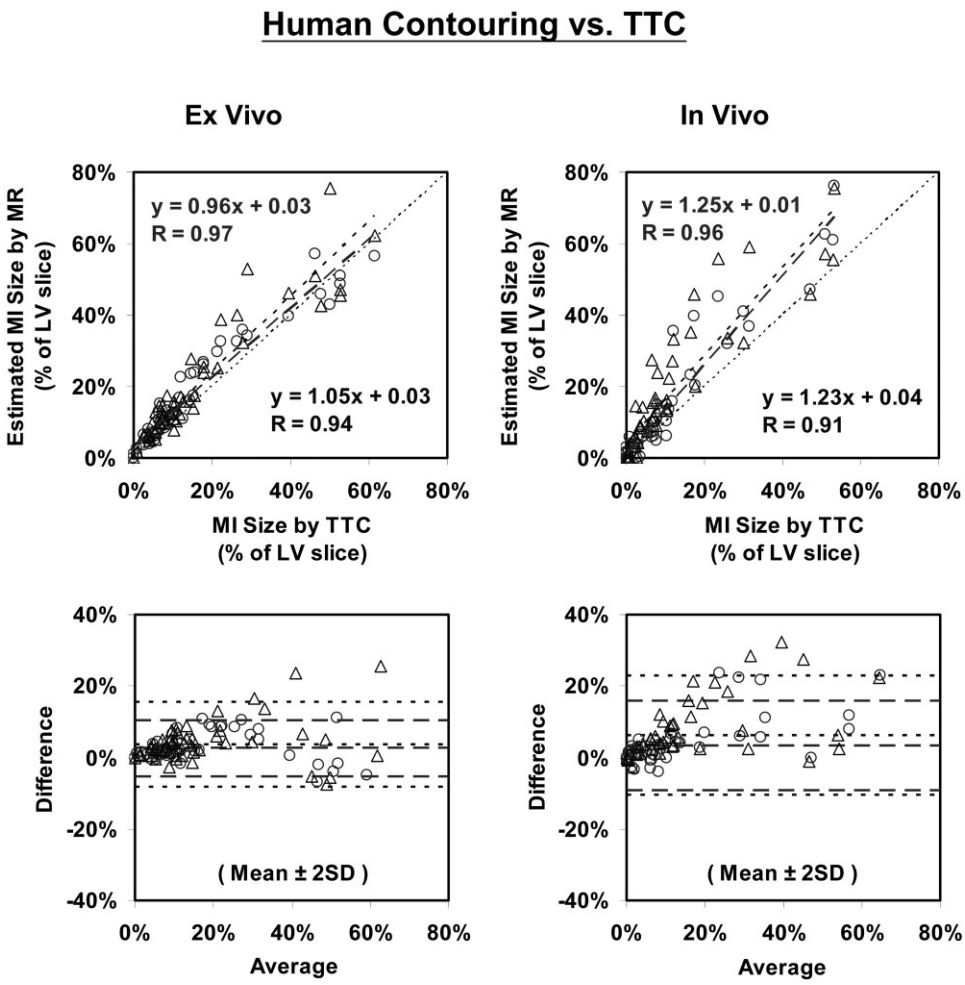

Figure 6. Despite good correlations between MR and TTC infarct size as measured by human manual contouring, Bland-Altman analysis shows systematic overestimation on MR images (intermodality comparison, MR vs. TTC). The first and second observers are indicated in open circles (dashed line) and triangles (dotted line), respectively.

vs. TTC) when manually tracing the infarct size on ex vivo images. This difference was even smaller using the FACT algorithm (0.2% of the LV, or 1.8% of the MI area, *P* not significant vs. TTC).

The difference between the two observers' manual contouring of in vivo images was considerably larger (4.0% of the LV, or 41.2% of the MI area, $P < 0.001$ vs. TTC). These interobserver differences were reduced more than 10 fold by using the FACT algorithm (0.3% of the LV, or 2.9% of the MI area, *P* not significant vs. TTC).

Both intraobserver and interobserver agreement on classifying pixels as infarcted generally showed excellent agreement (kappa > 0.8) on ex vivo and in vivo MR images (Table 1). However, human manual contouring tended to overestimate the number of infarcted pixels as evidenced by more pixels designated by human contouring but not the FACT algorithm. The interobserver agreement of myocardial segmentation was excellent (kappa > 0.9) on both ex vivo and in vivo MR images.

Comparisons of FACT Algorithm Vs. Simple Intensity Thresholding Techniques

For the group data overall, the FWHM intensity thresholding produced a smaller error than the 2SD intensity thresholding (Fig. 8). However, the FACT algorithm further reduced the error compared to both 2SD and FWHM intensity thresholding techniques ($P < 0.001$ and $P = 0.007$). This was true on both ex vivo and in vivo MR to TTC validations.

The results of infarct size measurements by the FACT algorithm, human manual contouring, and simple intensity thresholding based on 2SD and FWHM were summarized (Table 2). While human contouring of infarct size on MR was similar to the FWHM intensity thresholding, both had a smaller error than the 2SD intensity thresholding. The FACT algorithm however produced the smallest error compared to all other methods.

DISCUSSION

While MR acquisition methods have markedly improved image quality (3), quantitative analysis methods must be established that measure MI objectively and accurately on in vivo images. It is important to distinguish the current paper from prior validation studies (1,2) that aimed to prove gadolinium distribution differentiates normal myocardium from MI—a question answered by high resolution ex vivo images. The current study takes on the difficult task of accomplishing a higher accuracy in measuring infarct size, particularly on images obtained at clinically relevant image resolution. The systematic errors of infarct size measured by human manual contouring and simple intensity

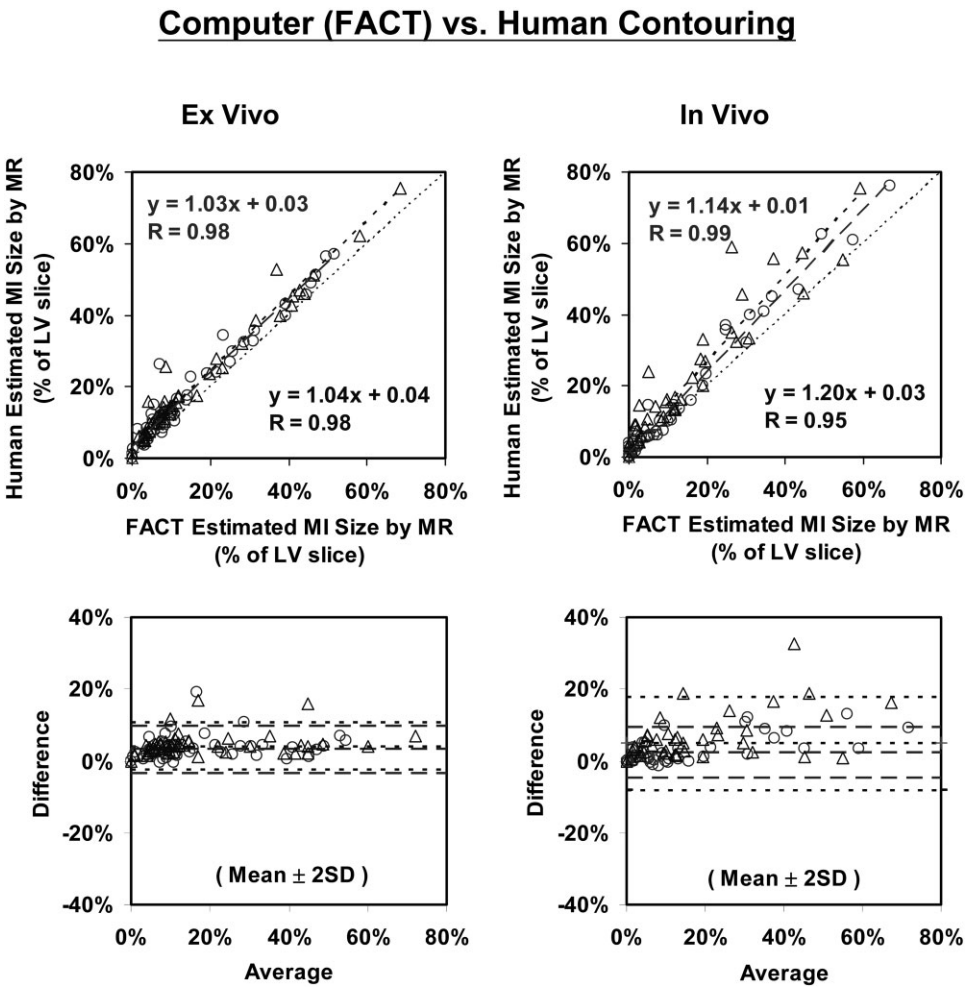

Figure 7. There are even tighter correlations when comparing infarct size measured by the FACT algorithm and human manual contouring on the same MR images (intramodality comparisons, MR vs. MR). Bland Altman analysis shows a trend of overestimation on human contouring. The first and second observers are indicated in open circles (dashed line) and triangles (dotted line), respectively.

thresholding as delineated in this paper do not question the accuracy of gadolinium-enhanced infarct imaging. Rather, this study indicates that infarct size can be determined accurately using delayed enhancement techniques at practical in vivo resolutions with the assistance of computerized methods that incorporate expert knowledge as the FACT algorithm presented in this study.

Table 1
Kappa Statistics for Pixel-Wise Comparison of Intraobserver and Interobserver Agreement on MR Images

	Ex vivo	In vivo
Intraobserver[a]		
Observer 1 infarct classification	0.83	0.86
Observer 2 infarct classification	0.83	0.80
Interobserver[b]		
Human infarct classification	0.79	0.87
Computer (FACT) infarct classification	0.81	0.90
Myocardial segmentation[c]	0.91	0.92

[a]Intraobserver comparisons of infarct classification describe the agreement between human contouring and the FACT algorithm for each observer.
[b]Interobserver comparisons of infarct classification indicate how well the two observers agreed in classifying pixels using a given method (human contouring or the FACT algorithm).
[c]Interobserver comparison of myocardial segmentation shows the agreement of two observers contouring myocardial regions.

Several factors can lead to systematic errors in quantifying infarct size even if the gadolinium concentrations accurately reflect the underlying pathology. These include partial volume errors, imperfect myocardial segmentation, inconsistencies introduced by different display setup or intensity thresholds, differences related to human visual perception, bright imaging artifacts on the myocardium, and dark but infarcted pixels due to microvascular obstruction (19). The proposed FACT algorithm takes into account all of these issues, though some of the sources of error warrant further discussion.

Another potential source of infarct sizing error is the inclusion of the peri-infarction zone, which results in intermediate pixel intensities (20). The peri-infarction zone can affect several pixels near the infarct borders and thus can lead to larger measurement errors than might be predicted by image resolution and an assumption of smooth infarct borders. It is likely that these peripheral zones are more difficult for a human to correctly quantify than a computer algorithm. Since the infarct territory exhibits a wavefront phenomenon (21), pixels that are further away from the core of the infarct are more likely to have increasing numbers of viable cells than those on the borders.

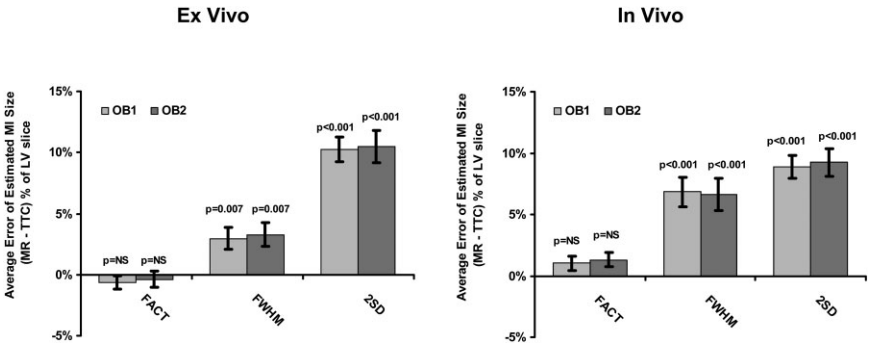

Figure 8. The FACT algorithm reduces average errors in measuring infarct size compared with simple intensity thresholding methods based on 2SD and FWHM. Both 2SD and FWHM methods significantly overestimate MR infarct size compared to TTC.

The FACT algorithm accurately measured infarct size on both ex vivo and in vivo MR images and reduced interobserver variability in our studies. In comparison, human manual contouring systematically overestimated in vivo infarct size despite a better ex vivo measurements. We suggest this is due to the finer resolution of the ex vivo images that have 12× smaller pixel volume (voxel) size and reduced tissue partial volume effects.

Partial volume issues warrant further discussion. Although TTC is the reference standard for determining infarct territory, TTC stains the surface of the myocardial slice and thus is not a volumetric measurement unless an infinite number of slices are studied. Nonetheless, thick MR slices introduce the possibility of a mixture of infarcted myocardium and normal myocardium within an image pixel as illustrated by Kim et al (1). This leads to a signal intensity that is brighter than completely normal myocardium but not quite bright enough to qualify as infarct. By analogy, it is known that the peri-infarction zone contains mixed populations of viable and nonviable tissues as well as edema (20). Such a combination of factors may result in intermediate contrast enhancement that requires an objective criterion to dichotomize normal from infarct pixels.

Ideally, viability could be assessed at the cardiomyocyte level. Based on the volume within a pixel (voxel), each ex vivo MR pixel represents on the order of 10,000 to 20,000 cardiomyocytes while the in vivo resolution is about 10 times worse. If a pixel contains 60% viable and 40% nonviable cardiomyocytes, it is reasonable to classify that pixel as viable even though it appears brighter than a completely normal pixel. This concept led us to use a 50% maximum intensity threshold (FWHM) to classify myocardial pixels within the limits that the pixel is essentially a mixture of a large number of cells.

While quantitative analyses using interactive intensity thresholding may reduce intraobserver or interobserver variability (8), these techniques lack robustness due to empirical threshold setting and may overestimate infarct size by inclusion of all bright pixels. We showed the use of FWHM intensity thresholding, which is based on contrast-enhanced pixels, as opposed to the threshold based on 2 SD that models the normal myocardium, can more accurately dichotomize normal from infarcted border tissues. We also demonstrated with high statistical certainty that the simple intensity thresholding methods used in most validation papers (1,2,7–13) overestimated infarct size on images acquired at in vivo resolutions compared to the FACT algorithm (Fig. 8).

It is interesting to note that the average errors of simple intensity thresholding based on 2SD and FWHM in our in vivo study (Table 2), when reported as percent of LV, were very similar to a recent report (13) using simple intensity thresholding for infarct sizing. Furthermore, the average error of human manual contouring in our study was comparable to the FWHM simple intensity thresholding (Table 2). This suggests that although human contouring can be as accurate as FWHM criteria, the accuracy of infarct size measurement can still be improved by using the FACT algorithm.

The region-based feature analysis of the FACT algorithm used expert derived rules to reduce type-II misclassification errors (false positive; overestimation) that occurred with simple thresholding techniques. The benefit of image feature analysis is most evident for eliminating epicardial white patches, such as right ventricular blood, that are included within imperfectly drawn epicardial borders. It can also exclude small isolated bright regions that result from imaging noise or potential artifacts provided they were not connected in three-dimensional space with other areas of infarction. Furthermore, feature analysis can designate dark pixels corresponding to microvascular obstruction.

In our canine validation, the FACT algorithm performed well on slices without infarction, which includes one animal with no TTC evidence of infarction. The segmentation of epicardial and endocardial borders by human readers was the first step for computer analysis,

Table 2
Summary of Average MR Infarct Sizing Errors Using Different Methods[a]

	Error in % of LV		Error in % of MI	
	Ex vivo	In vivo	Ex vivo	In vivo
FACT	0.5%	1.2%	3.5%	11.9%
Human	3.2%	5.4%	22.2%	55.1%
FWHM	3.1%	6.7%	21.8%	69.0%
2SD	10.4%	9.1%	72.2%	93.0%

[a]Errors are expressed as % of LV and % of MI for the difference between MR and TTC measurements.
FACT = Feature analysis and combined thresholding, Human = human manual contouring, FWHM = full width at half maximum intensity thresholding, 2SD = two–standard deviation intensity thresholding.

a potential source of subjective errors. In our results, interobserver agreement (kappa > 0.9) was excellent for myocardial segmentation (Table 1). The residual errors in the FACT algorithm infarct quantification suggested the difference in myocardial segmentation was not a major source of error.

The ability of inversion recovery and gadolinium-enhanced MR techniques to suppress the signal of normal myocardium leads to high contrast between normal and infarcted tissues (3). However, the accuracy of determining thresholds for infarct quantification based on simple image intensity, including FWHM approach (13), can be limited by noise bias (22) in conventional root-sum-square magnitude images unless PSIR reconstruction (14) is used. In addition, the use of FWHM criteria is based on the assumption that the MI contour is at 50% of the maximum intensity and not altered by the surface coil profile. Surface coil intensity correction is thus an important aspect for accurate MI sizing, particularly with large infarcts. The proposed FACT infarct sizing algorithm is now validated on the PSIR method but it can be extended to magnitude reconstruction achieving a similar accuracy as long as normal myocardium is properly nulled (23). Since PSIR imaging has benefits of being insensitive to inversion time and improved contrast-to-noise ratio compared to magnitude reconstruction, this algorithm may be further exploited over a relatively wide range of inversion recovery times for accurate myocardial infarct sizing.

Limitations

The algorithm was designed to identify necrosis that includes a subendocardial component as typically seen in patients with myocardial infarction due to coronary artery disease. Other etiologies of necrosis/fibrosis such as hypertrophic cardiomyopathy, cocaine induced infarction, and myocarditis may require modifications to the algorithm as these other diseases may cause fibrosis in other parts of the LV myocardium without affecting the subendocardium.

CONCLUSION

In conclusion, this paper presents a FACT algorithm that automatically selects optimal thresholds and uses feature analysis methods to classify normal and infarcted myocardium. It includes histopathological validations and indicates that in vivo MR accurately depicts the infarct region. The proposed algorithm measures infarct size more precisely than human manual contouring and simple intensity thresholding methods. Detailed validations were performed against histopathology in a canine infarct model including intraobserver and interobserver analysis to support these conclusions. The FACT algorithm improves the correlation, decreases random errors, minimizes intraobserver and interobserver variability, and reduces systematic overestimation that plagues human manual measurements or conventional simple intensity thresholding techniques. This computer-assisted methodology appears promising for serial infarct sizing in clinical and basic science studies.

ACKNOWLEDGMENTS

The authors thank Christine H. Lorenz, PhD, Siemens Corporate Research, Princeton, NJ, for many helpful suggestions regarding the method and study design.

REFERENCES

1. Kim RJ, Fieno DS, Parrish RB, et al. Relationship of MRI delayed contrast enhancement to irreversible injury, infarct age, and contractile function. Circulation 1999:100:1992–2002.
2. Fieno DS, Kim RJ, Chen EL, Lomasney JW, Klocke FJ, Judd RM. Contrast-enhanced magnetic resonance imaging of myocardium at risk: distinction between reversible and irreversible injury throughout infarct healing. J Am Coll Cardiol 2000:36:1985–1991.
3. Simonetti OP, Kim RJ, Fieno DS, et al. An improved MR imaging technique for the visualization of myocardial infarction. Radiology 2001:218:215–223.
4. Goldman MR, Brady TJ, Pykett IL, et al. Quantification of experimental myocardial infarction using nuclear magnetic resonance imaging and paramagnetic ion contrast enhancement in excised canine hearts. Circulation 1982:66:1012–1016.
5. Judd RM, Lugo-Olivieri CH, Arai M, et al. Physiological basis of myocardial contrast enhancement in fast magnetic resonance images of two-day old reperfused canine infarcts. Circulation 1995: 92:1902–1910.
6. Kim R, Chen E-L, Lima JAC, Judd RM. Myocardial Gd-DTPA kinetics determine MRI contrast enhancement and reflect the extent and severity of myocardial injury following acute reperfused infarction. Circulation 1996:94:3318–3326.
7. Lund GK, Stork A, Saeed M, et al. Acute myocardial infarction: evaluation with first-pass enhancement and delayed enhancement with MR imaging compared with 201ST1 SPECT imaging. Radiology 2004:232:49–57.
8. Setser RM, Bexell DG, O'Donnell TP, et al. Quantitative assessment of myocardial scar in delayed enhancement magnetic resonance imaging. J Magn Reson Imaging 2003:18:434–441.
9. Kim RJ, Wu E, Rafael A, et al. The use of contrast-enhanced magnetic resonance imaging to identify reversible myocardial dysfunction. N Engl J Med 2000:343:1145–1453.
10. Hillenbrand HB, Kim RJ, Parker MA, Fieno DS, Judd RM. Early assessment of myocardial salvage by contrast-enhanced magnetic resonance imaging. Circulation 2000:102:1678–1683.
11. Mahrholdt H, Wagner A, Holly TA, et al. Reproducibility of chronic infarct size measurement by contrast-enhanced magnetic resonance imaging. Circulation 2002:106:2322–2327.
12. Perin EC, Silva GV, Sarmento-Leite R, et al. Assessing myocardial viability and infarct transmurality with left ventricular electromechanical mapping in patients with stable coronary artery disease: validation by delayed-enhancement magnetic resonance imaging. Circulation 2002:106:957–961.
13. LC Amado, BL Gerber, SN Gupta, et al. Accurate and objective infarct sizing by contrast-enhanced magnetic resonance imaging in a canine myocardial infarction model. J Am Coll Cardiol 2004:44: 2383–2389.
14. Kellman P, Arai AE, McVeigh ER, Aletras AH. Phase sensitive inversion recovery for detecting myocardial infarction using Gadolinium delayed hyperenhancement. Magn Reson Med 2002:47:362–383.
15. Gonzalez RC, Woods RE. Digital image processing. Reading, MA: Addison Wesley; 1992.
16. Shrout PE, Fleiss JL. Intraclass correlations: uses in assessing rater reliability. Psychol Bull 1979:86:420–428.
17. Bland JM, Altman DG. Statistical methods for assessing agreement between two methods of clinical measurement. Lancet 1986:1:307–310.

18. Cohen J. A coefficient of agreement for nominal scales. Educational and Psychological Measurement 1960:20:37–46.
19. Wu K, Zerhouni EA, Judd RM, et al. The prognostic significance of microvascular obstruction by magnetic resonance imaging in patients with acute myocardial infarction. Circulation 1998:97:765–772.
20. Saeed M, Lund G, Wendland MF, Bremerich J, Weinmann H, Higgins CB. Magnetic resonance characterization of the peri-infarction zone of reperfused myocardial infarction with necrosis-specific and extracellular nonspecific contrast media. Circulation 2001: 103:871–876.
21. Reimer KA, Lowe JE, Rasmussen MM, Jennings RB. The wavefront phenomenon of ischemic cell death: myocardial infarct size vs. duration of coronary occlusion in dogs. Circulation. 1977:56:786–794.
22. Constantinides CD, Atalar E, McVeigh ER. Signal-to-noise measurements in magnitude images from NMR phased arrays. Magn Reson Med 1997;38:852–857.
23. Hsu L, Kellman P, Natanzon A, Aletras AH, Arai AE. Computer quantification of myocardial infarction on contrast enhanced magnetic resonance imaging. In: Proceedings of the 12th Annual Meeting of ISMRM, Kyoto, Japan, 2004.